

Inelastic scattering in ferromagnetic and antiferromagnetic metal spintronics

R.A. Duine,^{1,2,*} P.M. Haney,^{2,†} A. S. Núñez,^{3,2,‡} and A.H. MacDonald^{2,§}

¹*Institute for Theoretical Physics, Utrecht University,
Leuvenlaan 4, 3584 CE Utrecht, The Netherlands*

²*The University of Texas at Austin, Department of Physics,
1 University Station C1600, Austin, TX 78712-0264*

³*Instituto de Física, PUCV Av. Brasil 2950, Valparaíso, Chile*

(Dated: March 23, 2022)

We use a ferromagnetic voltage probe model to study the influence of inelastic scattering on giant magnetoresistance and current-induced torques in ferromagnetic and antiferromagnetic metal spin valves. The model is based on the Green's function formulation of transport theory and represents spin-dependent and spin-independent inelastic scatterers by interior voltage probes that are constrained to carry respectively no charge current and no spin or charge current. We find that giant magnetoresistance and spin transfer torques in ferromagnetic metal spin valve structures survive arbitrarily strong spin-independent inelastic scattering, while the recently predicted analogous phenomena in antiferromagnetic metal spin valves are partially suppressed. We use toy-model numerical calculations to estimate spacer layer thickness requirements for room temperature operation of antiferromagnetic metal spin valves.

PACS numbers:

I. INTRODUCTION

Electronic phase coherence often plays an important role in mesoscopic quantum transport. The simplest example, perhaps, is the Aharonov-Bohm effect¹ in a mesoscopic ring which is manifested by dependence of conductance on enclosed magnetic flux and requires phase coherence across the ring. In the Landauer-Büttiker theory of quantum transport^{2,3} it is possible to simulate phase breaking scattering processes by including internal 'floating' voltage probes in addition to source and drain⁴ electrodes, and requiring that their chemical potentials adjust so that they do not carry a current. This simple model is compatible with a Green's function description of transport and is able to describe those qualitative consequences of inelastic scattering not associated with the peculiarities of a specific mechanism. It has, for example, been applied to study the influence of phase decoherence on spin-independent transport in one-dimensional systems^{5,6}, and the effect of dephasing on transport through quantum dots^{7,8}.

In this paper we report on a comparison of the influence of inelastic scattering on giant magnetoresistance (GMR) and spin-transfer (ST) torque effects in traditional spin-valve structures containing ferromagnetic metals, and in the antiferromagnetic spin-valve structures that we^{9,10} have recently proposed. (Spin-valves are illustrated schematically in Fig. 1.) These devices are normally intended for operation at room temperature and above and electron scattering is therefore normally dominantly inelastic. In traditional ferromagnetic spin-valves only spin-flip scattering in the paramagnetic spacer is expected to have a large impact on GMR^{12,13} or ST^{14,15}. Both effects are expected to be strong when the spin diffusion length is longer than the paramagnetic spacer thickness. (Spin-independent in-

elastic scattering does however play a role in limiting the amplitude of oscillations in the dependence of exchange coupling between ferromagnetic layers on spacer layer thickness¹⁶.) It is commonly believed that GMR and ST in ferromagnetic spin-valves can survive arbitrarily strong spin-independent inelastic scattering. For antiferromagnetic spin-valves, however, the analogous effects depend⁹, at least in a simple toy model, on coherent multiple-scattering in the spacer layer and at its interfaces with the antiferromagnets. We have therefore argued that both effects will become weak when inelastic scattering is strong, even if the scattering is spin-independent. Since phonon scattering is only weakly spin-dependent and strong at high temperatures, inelastic scattering cannot be ignored in practical antiferromagnetic spin valves.

To pursue these ideas more quantitatively we use a voltage probe model to represent the influence of spin-independent and spin-dependent inelastic scatterers in a Green's function description of transport through a spin valve. In the linear response regime the voltage probe model has been shown to be equivalent to local coupling to a harmonic-oscillator heat bath¹⁷. In a magnetic metal circuit, however, conventional voltage probe models produce both longitudinal and transverse spin relaxation. Consider for example a largely collinear magnetic configuration with a natural spin-quantization axis. Spin components transverse to this axis are represented in quantum mechanics by coherence between spin-up and spin-down projections of the form $|\uparrow\rangle + e^{i\phi}|\downarrow\rangle$. A conventional paramagnetic voltage probe will change the magnitude and randomize the phase of both $|\uparrow\rangle$ and $|\downarrow\rangle$ parts of this spinor independently and therefore alter all spin-density components. This property was used very recently by Michaelis and Beenakker to model spin decay in chaotic quantum dots¹¹. This feature is however

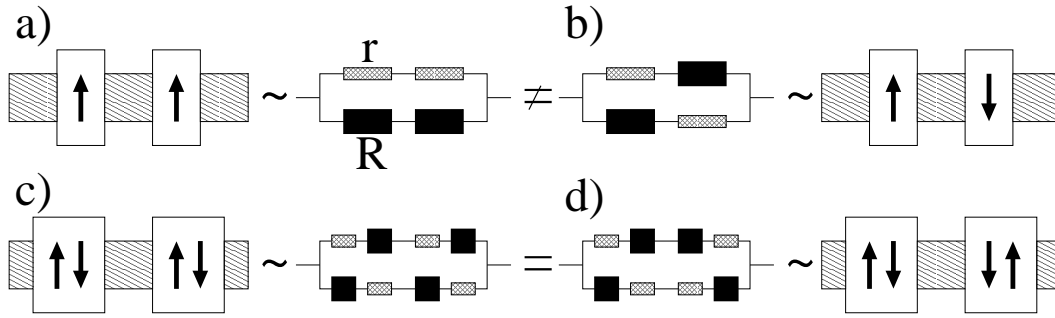


FIG. 1: a) Parallel configuration and equivalent circuit consisting of two resistors R and $r < R$, and b) antiparallel configuration and equivalent circuit, of a spin valve consisting of two single-domain ferromagnets separated by a paramagnetic spacer. c) Antiparallel configuration and equivalent circuit of an antiferromagnetic spin valve and d) its parallel configuration and equivalent circuit. (For convenience, only two ferromagnetic layers within each antiferromagnet are shown.) Note that in the ferromagnetic case the resistance of parallel and antiparallel circuits is different, contrary to the equivalent circuits in the antiferromagnetic case.

undesirable in modelling the influence of inelastic scattering on magnetoresistance properties of spintronic devices, because the strongest inelastic scatterers are often phonons, and phonons conserve spin to a good approximation. In our calculations we therefore use a voltage probe model generalized to the case of ferromagnetic probes, shown in Fig. 2. This generalization allows us to

consider separately spin-dependent and spin-independent inelastic scatterers. The spin-independent case is realized by adjusting the magnetization direction and the majority and minority spin chemical potentials of the voltage probes so that the probe carries neither charge or spin currents.

There are a number of important distinctions between GMR and ST physics in ferromagnetic and antiferromagnetic⁹ structures. In the ferromagnetic case GMR can be understood qualitatively simply by using a two-channel resistor model illustrated in Fig. 1 which does not rely on phase coherence. When applied to antiferromagnetic spin valves, the same argument does not predict GMR because the two spin channels have identical conductances (see Fig. 1. Clearly the antiferromagnetic spin-valve GMR effect relies at least in part on phase-coherence near the spacer layer as. In the simple model we discuss below antiferromagnetic spin-valve GMR comes about, roughly speaking, because the reflection amplitude for an electron scattering off an antiferromagnet is spin dependent, although the reflection probability and transmission amplitude and probability are not. Similarly ferromagnetic spin-valve ST torques can be understood by using a model of a ferromagnetic metal which has quasiparticle and magnetization orientation degrees of freedom, and appealing to conservation of total spin angular momentum to infer an action-reaction relationship between the torque exerted on the quasiparticles by the exchange field and the torque exerted on the magnetization by current-carrying quasiparticles. In the antiferromagnetic case, it is the staggered moment antiferromagnetic order which behaves collectively. Since this

coordinate does not carry total spin, its current-driven dynamics is not specified by a global conservation law. The theory of current-driven order parameter dynamics in this case requires a more microscopic approach¹⁸ in which ST is seen as following from changes in the spin-dependent exchange potential experienced by all quasiparticles, which follow in turn from changes in the spin-density in the presence of a transport current. Indeed the use of the term *spin transfer* torque is perhaps inappropriate in the antiferromagnetic case since current-induced order parameter changes *are not* related to transfer of total spin angular momentum between subsystems. Nevertheless staggered torques *do* act on the staggered spins and *do* drive the antiferromagnetic order parameter. To make clear that current-induced order parameter changes in antiferromagnets are not related to conservation of spin and are therefore strictly speaking not an example of spin transfer we, from now on, will call these torques *current-induced torques* (CIT's). Remarkably, current-induced torques in an antiferromagnetic spin-valve act throughout the volume of the antiferromagnets in the absence of inelastic scattering and disorder. Critical currents for order parameter reversal are therefore independent of antiferromagnetic film thickness in this limit, rather than being inversely proportional to thickness as in the ferromagnetic case.

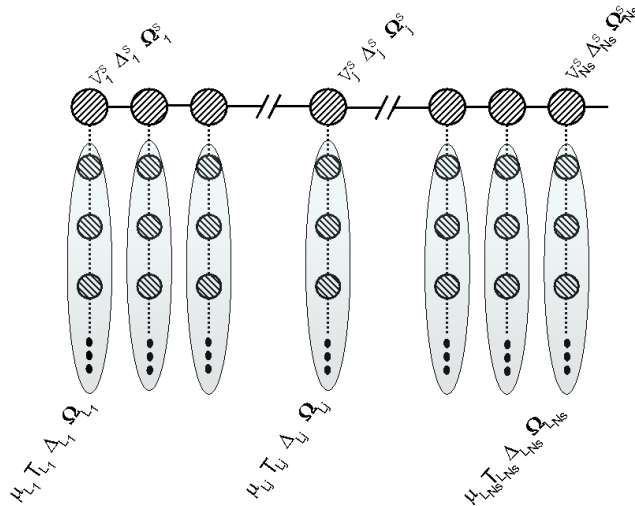


FIG. 2: Model system consisting of sites with an arbitrary onsite exchange potential. In addition to the coupling to its nearest neighbors, each site is coupled to a ferromagnetic reservoir.

The main aim of this paper is to shed light on the robustness of these GMR and current-induced torques in realistic room-temperature thin-film antiferromagnetic spin-valve structures by examining how properties change upon introduction of spin-dependent and spin-independent inelastic scatterers. The ferromagnetic voltage probe models of elastic and inelastic scattering are completely satisfactory for this purpose because we are interested in achieving a qualitative understanding that transcends the details of specific systems. We solve the model using the Green's function formalism for electronic transport in mesoscopic systems^{19,20}. This is convenient because the spin-torques we want to evaluate can be expressed¹⁸ in terms of the transport steady-state electron spin density and local observables are readily calculated using the Green's function formalism.

Our paper is organized as follows. In Sec. II we describe the Green's function formalism for electronic

transport as applied to systems with ferromagnetic leads. (For related work see Refs. [21] and Ref. [22].) The main result of this section is a general expression for the spin current from the ferromagnetic leads into the system which is necessary to apply our voltage probe model of a spin-independent inelastic scatterer. In Sec. III we apply the formalism to study the effect of spin-independent and spin-dependent inelastic scattering on magnetoresistance and current-induced torques in both ferromagnetic and antiferromagnetic systems. We conclude that although GMR and current-induced torques in antiferromagnetic spin-valves will be weakened by the inelastic scattering always present at spintronic device operation temperatures, the effects predicted in Ref. [9] should still be easily observable in favorable materials. We end in Sec. IV with a discussion of our results and some suggestions for future work.

II. GREEN'S FUNCTION FORMALISM WITH FERROMAGNETIC LEADS

In this section we describe our model system and give an expression for the spin current from the leads into the system.

A. Model

We consider first a one-dimensional non-interacting electron system that is connected on every site j to a fer-

romagnetic reservoir at equilibrium with chemical potential μ^j (see Fig. 2). The non-interacting electrons should be understood as quasiparticles in a mean-field description of a magnetic metal similar to the Kohn-Sham quasiparticles of spin-density functional theory. The assumption of one-dimensionality is not essential. Calculations similar to the ones we describe which allow for a number of transverse channels could be carried out to model particular materials systems realistically. The generalization of the formalism to two and three dimensions is straightforward. The total Hamiltonian $\mathcal{H} = \mathcal{H}_S + \mathcal{H}_L + \mathcal{H}_C$ is the sum of three parts. The first term describes the sys-

tem, which in our case includes the paramagnetic spacer layer and the magnets. In terms of the second-quantized operators $\hat{c}_{j,\sigma}$ that annihilate an electron in spin state $\sigma \in \{\uparrow, \downarrow\}$ at site j

$$\begin{aligned} \mathcal{H}_S = & -J_S \sum_{\langle j,j' \rangle; \sigma} \hat{c}_{j,\sigma}^\dagger \hat{c}_{j',\sigma} \\ & + \sum_{j;\sigma,\sigma'} \hat{c}_{j,\sigma}^\dagger (V_j^S \delta_{\sigma,\sigma'} - \Delta_j^S \mathbf{\Omega}_j^S \cdot \boldsymbol{\tau}_{\sigma,\sigma'}) \hat{c}_{j,\sigma'} . \end{aligned} \quad (1)$$

In this expression the first term is proportional to the hopping amplitude J_S and its sum is over nearest neighbors only. In the second and third terms of \mathcal{H}_S we allow for a site-dependent scalar potential V_j^S and a site-dependent exchange potential $-\Delta_j^S \mathbf{\Omega}_j^S$ where $\mathbf{\Omega}_j^S$ is a unit vector which specifies the (instantaneous) magnetization orientation on site j and $\boldsymbol{\tau}$ is the Pauli spin-matrix vector. This single-particle Hamiltonian should be understood as a time-dependent mean-field Hamiltonian that depends on the instantaneous $\mathbf{\Omega}_j^S$ values. We assume that the magnetization dynamics is always slow enough to justify time-independent quasiparticle transport theory. The leads are described by the Hamiltonian $\mathcal{H}_L = \sum_j \mathcal{H}^{L_j}$, where \mathcal{H}^{L_j} is the Hamiltonian of the lead that is connected to the system at site j , which is given by

$$\begin{aligned} \mathcal{H}^{L_j} = & -J_{L_j} \sum_{\langle j',j'' \rangle; \sigma} \left[\hat{d}_{j',\sigma}^{L_j} \right]^\dagger \hat{d}_{j'',\sigma}^{L_j} \\ & - \Delta^{L_j} \mathbf{\Omega}^{L_j} \cdot \sum_{j';\sigma,\sigma'} \left[\hat{d}_{j',\sigma}^{L_j} \right]^\dagger \boldsymbol{\tau}_{\sigma,\sigma'} \hat{d}_{j',\sigma'}^{L_j} , \end{aligned} \quad (2)$$

where $\hat{d}_{j,\sigma}^{L_j}$ are the fermionic annihilation operators of the j -th lead and J_{L_j} is the hopping amplitude in that lead. Each lead has a chemical potential μ_j and a uniform exchange potential $-\Delta^{L_j} \mathbf{\Omega}^{L_j}$ which we adjust as described earlier to simulate spin-independent and spin-dependent inelastic scatterers. Note that $\mathbf{\Omega}^{L_j}$ is in general different for different leads. The Hamiltonian that couples the system and its leads is $\mathcal{H}_C = \sum_j \mathcal{H}_C^j$ where

$$\mathcal{H}_C^j = -J_C^j \sum_{\sigma} \left[\hat{c}_{j,\sigma}^\dagger \hat{d}_{\partial L_j,\sigma}^{L_j} + \left[\hat{d}_{\partial L_j,\sigma}^{L_j} \right]^\dagger \hat{c}_{j,\sigma} \right] . \quad (3)$$

Here, ∂L_j denotes the last site of the half-infinite ferromagnetic reservoir connected to site j , and J_C^j is the amplitude to hop from that reservoir to the system.

B. Quantum Transport Green's Function Formalism

The quantum transport Green's function formalism determines the equal-time "lesser" Green's function^{19,20} $G_{j,\sigma;j',\sigma'}^<(t,t) \equiv i \langle \hat{c}_{j',\sigma'}^\dagger(t) c_{j,\sigma}(t) \rangle$ of the system in the

transport steady state, the quantity in terms of which all observables are calculated. It is given by^{19,20}

$$-iG^<(t,t) \equiv \rho = \sum_j \int \frac{d\epsilon}{(2\pi)} N(\epsilon - \mu^j) A^j(\epsilon) , \quad (4)$$

where $N(x) = (e^{\beta x} + 1)^{-1}$ is the Fermi distribution function, $\beta = 1/k_B T$ the inverse thermal energy, and

$$A^j(\epsilon) = G^{(+)}(\epsilon) \hbar \Gamma^j(\epsilon) G^{(-)}(\epsilon) , \quad (5)$$

the spectral weight contribution from lead j . The matrix elements of the rate $\hbar \Gamma^j(\epsilon)$ are related to the retarded self energy of lead j , denoted by $\hbar \Sigma^{j,(+)}(\epsilon)$, by

$$\hbar \Gamma^j(\epsilon) = i \left[\hbar \Sigma^{j,(+)}(\epsilon) - \hbar \Sigma^{j,(-)}(\epsilon) \right] , \quad (6)$$

where $\hbar \Sigma^{j,(-)}(\epsilon)$ is the complex transpose of the retarded self energy. ($G^{(-)}$ is obtained similarly from the expression for $G^{(+)}$ below.) The only nonzero elements of the retarded self-energy are

$$\begin{aligned} \hbar \Sigma_{j,\sigma;j,\sigma'}^{j,(+)}(\epsilon) = & -\frac{(J_C^j)^2}{2J_{L_j}} \left[e^{ik_\uparrow^j(\epsilon)a} + e^{ik_\downarrow^j(\epsilon)a} \right] \delta_{\sigma,\sigma'} \\ & -\frac{(J_C^j)^2}{2J_{L_j}} \left[e^{ik_\uparrow^j(\epsilon)a} - e^{ik_\downarrow^j(\epsilon)a} \right] \mathbf{\Omega}^{L_j} \cdot \boldsymbol{\tau}_{\sigma,\sigma'} , \end{aligned} \quad (7)$$

where $k_\sigma^j(\epsilon) = \arccos[-(\epsilon + \sigma \Delta^{L_j})/2J_{L_j}]/a$ is the wave vector in the leads at energy ϵ , with a the lattice constant. Finally, the retarded Green's function is specified by

$$\left[\epsilon^+ - H - \sum_j \hbar \Sigma^{j,(+)}(\epsilon) \right] G^{(+)}(\epsilon) = 1 , \quad (8)$$

with $\epsilon^+ \equiv \epsilon + i0$ where the system Hamiltonian is

$$\begin{aligned} H_{j,\sigma;j',\sigma'} = & -J_S \delta_{\sigma,\sigma'} (\delta_{j,j'-1} + \delta_{j,j'+1}) \\ & + \delta_{j,j'} (V_j^S \delta_{\sigma,\sigma'} - \Delta_j^S \mathbf{\Omega}_j^S \cdot \boldsymbol{\tau}_{\sigma,\sigma'}) . \end{aligned} \quad (9)$$

Note that H , ρ , $G^<$, A^j , $\hbar \Gamma^j$, $\hbar \Sigma^{j,(\pm)}$ and $G^{(\pm)}$ are matrices in real and spin space of dimension $(2N_s) \times (2N_s)$, where N_s is the number of sites in the system. From now on we use the convention that any quantity is a matrix in those indices that are not explicitly indicated. For example, the quantity $G_{i,j}^{(+)}(\epsilon)$ is a 2×2 matrix in spin space.

We now proceed to calculate the current and spin currents from the leads into the system. Since the underlying model Hamiltonian in these model calculations are spin-rotationally invariant, each component of spin is conserved and there is no ambiguity in the spin-current definition. The expression for the current from lead j has been derived previously²³ and is given by

$$-\frac{dN^j}{dt} \equiv -\frac{d}{dt} \sum_{j',\sigma} \left\langle \left[\hat{d}_{j',\sigma}^{L_j} \right]^\dagger \hat{d}_{j',\sigma}^{L_j}(t) \right\rangle$$

$$= \frac{1}{\hbar} \int \frac{d\epsilon}{(2\pi)} \sum_k [N(\epsilon - \mu^j) - N(\epsilon - \mu^k)] \text{Tr} \left[\hbar \Gamma^j(\epsilon) G^{(+)}(\epsilon) \hbar \Gamma^k(\epsilon) G^{(-)}(\epsilon) \right]. \quad (10)$$

This expression relates the Landauer-Büttiker formalism to the Green's function formalism²⁴.

The expression for the spin current into lead j proceeds along similar lines. We first calculate the rate of change of spin-density in lead j :

$$\begin{aligned} \frac{ds^j}{dt} &\equiv \frac{d}{dt} \sum_{j'; \sigma, \sigma'} \left\langle \left[\hat{d}_{j', \sigma}^{L_j}(t) \right]^\dagger \frac{\tau_{\sigma, \sigma'}}{2} \hat{d}_{j', \sigma'}^{L_j}(t) \right\rangle \\ &= -\frac{iJ_C^j}{2\hbar} \sum_{\sigma, \sigma'} \tau_{\sigma, \sigma'} \left[\left\langle \hat{c}_{j, \sigma}^\dagger(t) \hat{d}_{\partial L_j, \sigma'}^{L_j}(t) \right\rangle - \text{c.c.} \right]. \end{aligned} \quad (11)$$

In principle, there is an additional term that describes the precession of electronic spins in the lead around the exchange field in the leads, but this term vanishes since the leads are assumed to be in equilibrium and assumed to have a spin that is aligned with the exchange field.

The evaluation of the above expression follows the same line as in the charge current expression derived by Meir and Wingreen²³. We first introduce the Green's function $G_{j; \sigma, \sigma'}^{C, <}(t, t') \equiv i \left\langle \left[\hat{d}_{\partial L_j, \sigma'}^{L_j}(t') \right]^\dagger \hat{c}_{j, \sigma}(t) \right\rangle$. The corresponding Keldysh contour ordered Green's function obeys the Dyson equation²³

$$G_j^C(t, t') = \frac{J_C^j}{\hbar} \int_{\mathcal{C}^\infty} dt'' G_{j, j}(t, t'') G_{\partial L_j, \partial L_j}^{L_j}(t'', t'), \quad (12)$$

where the time integration is over the Keldysh contour \mathcal{C}^∞ . In Eq. (12) $G(t, t')$ is the contour ordered Green's

function of the system coupled to the leads whereas, in order to avoid double-counting of the effects of coupling between system and leads, $G^{L_j}(t, t')$ is the contour ordered Green's functions for the j -th lead *in the absence* of coupling to the system. Using standard rules for calculus on the Keldysh contour we find that

$$\begin{aligned} G_j^{C, <}(t, t') &= \frac{J_C^j}{\hbar} \int dt'' \left[G_{j, j}^{(+)}(t, t'') G_{\partial L_j, \partial L_j}^{L_j, <}(t'', t') \right. \\ &\quad \left. + G_{j, j}^{<}(t, t'') G_{\partial L_j, \partial L_j}^{L_j, (-)}(t'', t') \right], \end{aligned} \quad (13)$$

which after Fourier transformation results in

$$\begin{aligned} G_j^{C, <}(\epsilon) &= J_C^j \left[G_{j, j}^{(+)}(\epsilon) G_{\partial L_j, \partial L_j}^{L_j, <}(\epsilon) \right. \\ &\quad \left. + G_{j, j}^{<}(\epsilon) G_{\partial L_j, \partial L_j}^{L_j, (-)}(\epsilon) \right]. \end{aligned} \quad (14)$$

This expression is evaluated using

$$G_{\partial L_j, \partial L_j}^{L_j, <}(\epsilon) = \frac{i}{\left(J_C^j\right)^2} N(\epsilon - \mu^j) \hbar \Gamma_{j, j}^j(\epsilon), \quad (15)$$

$$G_{\partial L_j, \partial L_j}^{L_j, (-)}(\epsilon) = \frac{1}{\left(J_C^j\right)^2} \hbar \Sigma_{j, j}^{j, (-)}(\epsilon), \quad (16)$$

and the kinetic equation [Eq. (4)] to obtain

$$\begin{aligned} G_j^{C, <}(\epsilon) &= \frac{i}{J_C^j} \left[N(\epsilon - \mu^j) G_{j, j}^{(+)}(\epsilon) \hbar \Gamma_{j, j}^j(\epsilon) \right. \\ &\quad \left. + \sum_k N(\epsilon - \mu^k) A_{j, j}^k(\epsilon) \hbar \Sigma_{j, j}^{j, (-)}(\epsilon) \right]. \end{aligned} \quad (17)$$

It follows that

$$\frac{ds^j}{dt} = \frac{1}{2\hbar} \int \frac{d\epsilon}{(2\pi)} \text{Tr} \left\{ N(\epsilon - \mu^j) \hbar \Gamma_{j, j}^j(\epsilon) i \left[\tau G_{j, j}^{(+)}(\epsilon) - G_{j, j}^{(-)}(\epsilon) \tau \right] - \sum_k N(\epsilon - \mu^k) i \left[\tau \hbar \Sigma_{j, j}^{j, (+)}(\epsilon) - \hbar \Sigma_{j, j}^{j, (-)}(\epsilon) \tau \right] A_{j, j}^k(\epsilon) \right\}. \quad (18)$$

In the next subsection we turn to a discussion of the physical content of this equation.

C. Spin-Currents, Exchange Interactions, and Current-Induced Torques

In order to provide some insight into the general expression we have derived for the spin-current, we examine first the relatively simple situation in which the system is connected to leads only on the most left and most right sites, denoted by site 1 and N_s respectively. Their respective chemical potentials are $\mu^1 = \epsilon_F + |e|V$, and

$\mu^{N_s} = \epsilon_F$ with $|e|V > 0$. Moreover, we assume that there is no exchange potential in the system, i.e., $\Delta_j^S = 0$, so that spin currents are conserved in the system. This is the circumstance then of transport between ferromagnetic leads through a paramagnetic system. In this case $ds^1/dt = -ds^{N_s}/dt$. It is informative to separate the spin-current flowing between leads into equilibrium and non-equilibrium contributions:

$$\frac{ds^1}{dt} = \left. \frac{ds^1}{dt} \right|_{\text{eq}} + \left. \frac{ds^1}{dt} \right|_{\text{neq}}. \quad (19)$$

It follows quite generally from the time-dependent Schroedinger equation satisfied by quasiparticles that

ds/dt has contributions from the spin-current divergence and from precession around an effective magnetic field. Since the leads are by definition spatially homogeneous, it follows that spin-currents in the leads may be equally well

thought of as a torque acting on the leads. The equilibrium spin-torque is given (at temperatures low compared to Fermi energies) by

$$\left. \frac{ds^1}{dt} \right|_{\text{eq}} = \frac{1}{2\hbar} \int_{-\infty}^{\epsilon_F} \frac{d\epsilon}{(2\pi)} \text{Tr} \left\{ \hbar \Gamma_{1,1}^1(\epsilon) i \left[\tau G_{1,1}^{(+)}(\epsilon) - G_{1,1}^{(-)}(\epsilon) \tau \right] - i \left[\tau \hbar \Sigma_{1,1}^{1,+}(\epsilon) - \hbar \Sigma_{1,1}^{1,-}(\epsilon) \tau \right] A_{1,1}(\epsilon) \right\}, \quad (20)$$

where $A(\epsilon) \equiv i [G^{(+)}(\epsilon) - G^{(-)}(\epsilon)]$ is the total spectral function. It can be shown that the equilibrium torque always points out of the plane spanned by $\mathbf{\Omega}^{L_1}$ and $\mathbf{\Omega}^{L_{Ns}}$, the magnetization directions of the two leads. This is expected, since the equilibrium contribution to the torques between the leads is a simply due to exchange coupling mediated by the paramagnetic system. The dynamics induced by this coupling conserves total energy and hence leaves $\mathbf{\Omega}^{L_1} \cdot \mathbf{\Omega}^{L_{Ns}}$ invariant. Note that spin currents are even under time reversal, unlike charge currents, and can be present in equilibrium.

The nonequilibrium (transport) contribution to the torques between the two leads, is given by

$$\left. \frac{ds^1}{dt} \right|_{\text{neq}} = \frac{1}{2\hbar} \int_{\epsilon_F}^{\epsilon_F + |e|V} \frac{d\epsilon}{(2\pi)} \text{Tr} \left\{ \hbar \Gamma_{1,1}^1(\epsilon) i \left[\tau G_{1,1}^{(+)}(\epsilon) - G_{1,1}^{(-)}(\epsilon) \tau \right] - i \left[\tau \hbar \Sigma_{1,1}^{1,+}(\epsilon) - \hbar \Sigma_{1,1}^{1,-}(\epsilon) \tau \right] A_{1,1}^1(\epsilon) \right\}, \quad (21)$$

and has both an out-of-plane and in-plane contribution. The former corresponds to a transport-modified electron-mediated exchange torque between the leads. The latter corresponds to the spin transfer torque between the ferromagnetic leads. (This contribution was also calculated within the context of the Green's function formalism in Ref. [21] for the case of two ferromagnetic leads.) Note that the in-plane spin transfer torque is present only at finite bias $|e|V$, which reflects the fact that energy-conservation violating torques can only be present in a nonequilibrium situation. Finally, note that this spin transfer torque acts on the leads and should not be confused with the torques that act on the local magnetization in the system that we calculate in the next section.

III. APPLICATIONS

The ferromagnetic voltage probe model discussed in the previous section is a flexible tool which can be used to model a wide variety of potentially interesting spintronic device geometries. We use it in this section to model both spin-independent and spin-dependent inelastic scattering.

In the presence of an exchange field which defines a preferred direction in spin space, we can recognize (at least) three different length scales that are relevant to spintronic device functionality. The phase-coherence length L_ϕ is the length over which electronic quasiparticles maintain phase coherence. The spin-flip scattering length or spin diffusion length L_{sf} is the average distance travelled along the channel between spin-flip scattering events. This quantity usually controls the length scale

on which the magnitude of the magnetization along the exchange field direction recovers local equilibrium, and therefore also the paramagnetic spacer layer thickness scale at which giant magnetoresistance effects are strongly attenuated. The spin-coherence length L_{sc} is the length scale over which components of the spin-density transverse to the exchange field can be maintained. The phase-coherence length is limited by spin-dependent inelastic scattering processes. In addition to this inelastic contribution, the spin-coherence length in two and three dimensional ferromagnetic metals tends to be short because of destructive interference due to the phase difference of the spinor components in transverse conduction channels²⁵ with different Fermi velocity components in the current flow direction. As we discuss below, phase coherence can have a strong influence on the properties of a spintronic circuit, especially in circuits containing antiferromagnetic elements.

The solution of transport Green's function models with ferromagnetic leads and non-collinear magnetization presents a number of numerical challenges, even for the one-dimensional case we consider here, because the spin and charge currents in the leads depend nonlinearly on both the magnetization direction and the magnitude of the exchange spin-splitting in each lead. When we wish to model a spin-independent inelastic scatterer, both the magnitude and the direction in each lead have to be carefully adjusted to achieve the zero-spin-current condition. Indeed the case of spin-independent inelastic scatterers can be very relevant to experiment since phonon-scattering can be dominant in experimental systems. To model circumstances in which phonon scattering is dominant ($L_{sf} \gg L_\phi$), we must deal with the com-

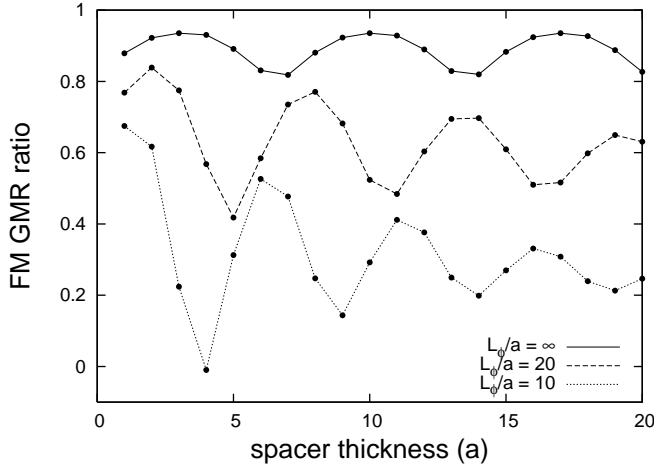


FIG. 3: Ferromagnetic GMR ratio as a function of the spacer thickness for various inelastic scattering lengths.

plications associated with preventing spin-relaxation in the voltage probes, a requirement that is especially troublesome for non-collinear magnetization configurations. Inelastic scattering off magnons, which does flip spins, can also be important however. The simplest case to examine numerically is one with paramagnetic, *i.e.* spin-isotropic, voltage probes. Calculations with this voltage probe model are relatively simple even for non-collinear magnetizations, since in this case only the charge current into the probes is set to zero. This limit corresponds to $L_{sf} = L_\phi$ and can be interpreted as representing the case in which quasiparticle scattering from magnons is dominant.

We start by considering the giant magnetoresistance (GMR) ratio which is easier to evaluate because we need to consider only parallel and antiparallel configurations which are both collinear. We define the GMR ratio as

$$\eta = \frac{G_P - G_{AP}}{G_P}, \quad (22)$$

where G_P is the conductance for the parallel configuration and G_{AP} for the antiparallel one. For antiferromagnets, the designations *parallel* and *antiparallel* refer to the moment directions on the two sites adjacent to the paramagnetic spacer.

In our model we define the phase coherence length as the product of the Fermi velocity and the inelastic scattering rate:

$$L_\phi = \frac{4J_S a \sin(k_F a)}{\hbar \text{Tr} \left[\sum_j \Gamma^j(\epsilon_F)/N_s \right]}, \quad (23)$$

where k_F is the Fermi wave length of the system. This definition is motivated the fact that the inelastic scattering time is given roughly by $2/\text{Tr} \left[\sum_j \Gamma^j(\epsilon_F)/N_s \right]$.

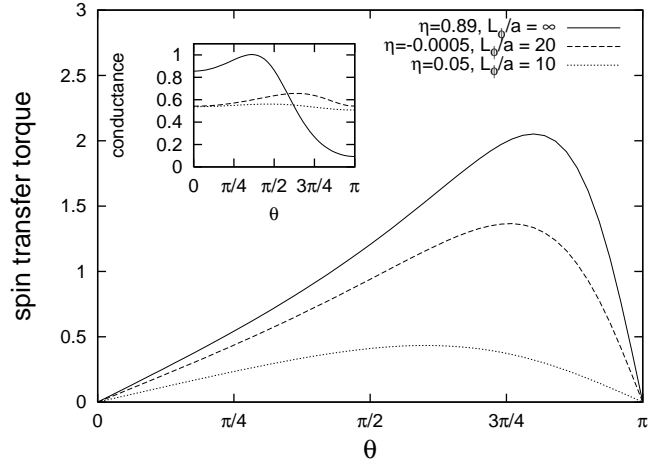


FIG. 4: Spin transfer torque for the case $L_{sf} = L_\phi$ normalized to $I/|e|$, where I is the charge current, as a function of θ . The inset shows the conductance in units of $|e|/(2\pi\hbar)$. For this calculation the spacer thickness is taken equal to 5 sites.

A. Ferromagnetic Metal Nanostructures

We report results for a spin-valve ferromagnetic nanostructure, which consists of two ferromagnetic elements separated by a paramagnetic spacer (See Fig. 1). This structure is known as a spin-valve because the current can be sharply reduced under favorable circumstances when the two ferromagnets have opposite orientations. In our toy model we choose $\Delta_j^S/J_S = 0.5$ and independent of position, *i.e.* the site index j , in the ferromagnetic parts of the system. In the paramagnetic parts the exchange potential is set to zero. Both ferromagnets are 4 sites long in our tight-binding model. The other parameters used for the calculations reported on here were $\epsilon_F/J_S = 1.8$, $J_S = J_{L_j}$ and V_j^S .

1. GMR ratio for $L_{sf} \gg L_\phi$

To model a finite phase coherence length due to spin independent inelastic scattering, the phonon scattering case, we choose $L_{sf} = \infty$. We then have to require that both spin and charge currents into the voltage probes vanish. As explained before, considering the non-collinear case for this situation is very difficult numerically. However, calculation of the GMR ratio requires comparing parallel and antiparallel configuration in which the spin currents with polarization out of the plane are zero. This observation makes calculating the GMR ratio numerically tractable.

In Fig. 3 we present results for the GMR ratio as a function of spacer thickness for various inelastic scattering lengths. The GMR ratio exhibits oscillations as a function of spacer thickness which have been observed experimentally¹⁶. For the phase coherent case these oscillations persist up to arbitrary large spacer thickness in

our one-dimensional model. For finite L_ϕ the oscillations are damped and the GMR ratio saturates to a nonzero value for a spacer of thickness much larger than L_ϕ . This is expected because for a ferromagnet the transmission and reflection probabilities are spin dependent, and not only the amplitudes.

2. GMR ratio and spin transfer torques for $L_\phi = L_{sf}$

For the magnon scattering case, $L_\phi = L_{sf}$, implemented by making the floating voltage probes paramagnetic and requiring the charge current to be zero, we are also able to consider the non-collinear case. The spin transfer torques are due to the net misalignment of electron spins with the local magnetization in the transport steady state¹⁸, and calculated from

$$\Gamma^{\text{st}} \equiv \sum_j \frac{\Delta_j^S}{\hbar} \Omega_j^S \times \langle \mathbf{s} \rangle_\perp. \quad (24)$$

Here, $\langle \mathbf{s} \rangle_\perp$ denotes the electron spin component that points out of the plane spanned by the two magnetizations. The sum over sites in the above expression is restricted to the ferromagnet for which we want to calculate the spin transfer torques, which in our case is by definition the right “downstream” ferromagnet. In Fig. 4 the spin transfer torque per current is shown for various L_ϕ as a function of the angle θ between the two ferromagnets. The inset of this figure shows the conductance as a function of this angle. Clearly, both GMR and spin transfer torques are suppressed for decreasing L_ϕ , as expected in the $L_{sf} = L_\phi$ case.

B. Antiferromagnetic Metal Nanostructures

In this subsection, we consider a system which consists of two antiferromagnets separated by a paramagnetic spacer. Hence, we take $\Delta_j^S = \Delta(-1)^j$ in the magnetic parts of the system, and zero in the paramagnetic parts. We take the parameters $\Delta/J_S = 1$. The other parameters used to obtain the results reported on here were $\epsilon_F/J_S = 1.8$, $J_S = J_{L_j}$, and V_j^S . The calculations presented in this subsection were performed on nanostructures in which each antiferromagnet has 30 sites.

1. GMR ratio for $L_{sf} \gg L_\phi$

In Fig. 5 the antiferromagnetic GMR ratio is shown as a function of the thickness of the spacer, for various inelastic scattering length L_ϕ . Note that as the phase coherence length decreases, the oscillations in the GMR ratio with increasing thickness are suppressed. Unlike the case of a ferromagnetic spin valve, the GMR ratio goes to zero when the thickness of the spacer is much larger than the phase coherence length. This property demonstrates

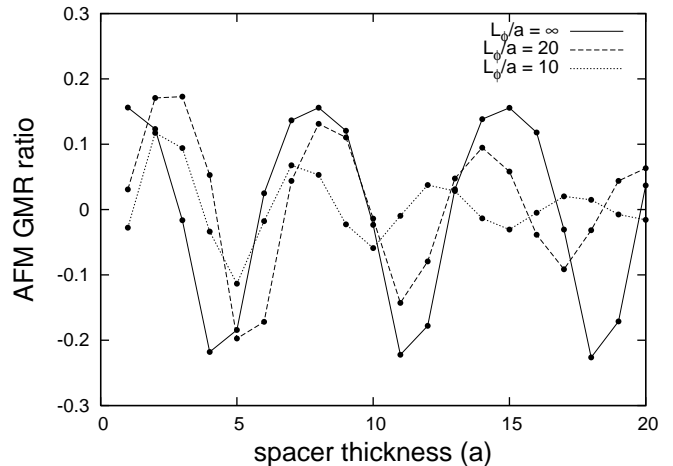


FIG. 5: Antiferromagnetic GMR ratio as a function of the spacer thickness for various inelastic scattering lengths.

that phase coherence is essential for the antiferromagnetic GMR effect. This observation is in agreement with qualitative arguments presented in previous work⁹. Note however, that the GMR decreases rather gradually with decreasing phase coherence length.

2. GMR and current-induced torques for $L_\phi = L_{sf}$

One of the most important results in our previous work on antiferromagnets⁹ is that in the ballistic limit the out of plane spin density which is responsible for the current-induced torque is periodic with the period of the antiferromagnet. For the tight-binding model used in this paper this property implies that this spin density component, present only in the transport steady state, is constant throughout the antiferromagnet. It is this property which makes current-induced torques very efficient in driving collective order parameter dynamics in uncompensated antiferromagnets in the absence of inelastic scattering.

In Fig. 6 we show the out of plane spin density for the angle $\theta = \pi/2$ between two moments in the antiferromagnets opposite the spacer. This calculation was performed for a spacer thickness of 10 sites. In agreement with our previous results we find that for $L_\phi = \infty$ the out of plane spin density is constant. For nonzero L_ϕ the out of plane spin density decays away from the spacer into the antiferromagnets.

In Fig. 7 we show the current-induced torque per current acting on the right antiferromagnet as a function of the angle θ between the two moments facing the paramagnetic spacer. It is important to realize that a single domain antiferromagnet is driven by a staggered torque. Hence, in this case we have to calculate the staggered torque given by

$$\Gamma^{\text{st}} \equiv \frac{1}{\hbar} \sum_j (-1)^j \Delta \Omega_j^S \times \langle \mathbf{s} \rangle_\perp. \quad (25)$$

As expected, both GMR and current-induced torques are

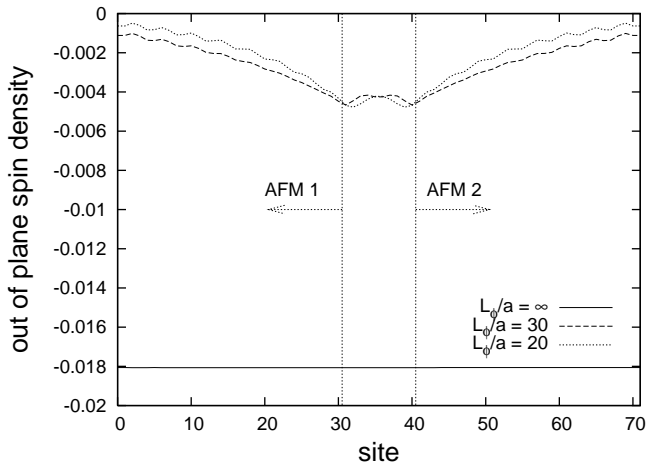


FIG. 6: Spin density component out of the plane spanned by the moments of the antiferromagnets opposite the paramagnetic spacer layer for various inelastic scattering lengths. In this calculation $L_\phi = L_{sf}$.

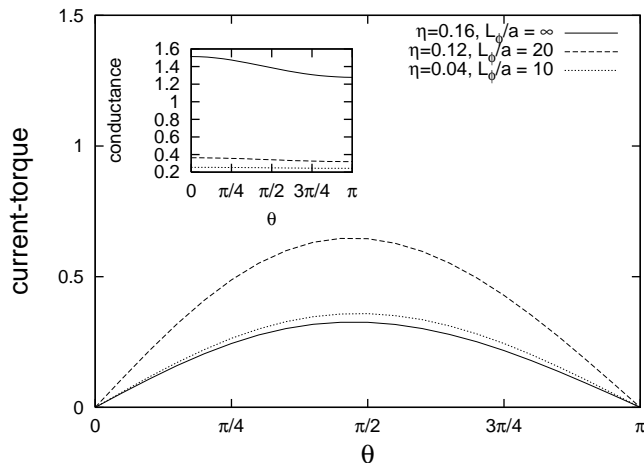


FIG. 7: Current-induced torques normalized to $I/|e|$, where I is the charge current, as a function of θ . The inset shows the conductance in units of $|e|/(2\pi\hbar)$. In this calculation $L_\phi = L_{sf}$ and the number of spacer sites is 4.

reduced by inelastic scattering. It is somewhat surprising that the current-induced torques at $L_\phi = 20$ are larger than at $L_\phi = \infty$. However, this is most likely because the current-induced torque is normalized to the current and because of the one-dimensional model under consideration. We checked that in the limit $L_\phi \rightarrow 0$ the current-induced torques always vanish.

IV. DISCUSSION AND CONCLUSIONS

The most important conclusion of this paper is that the introduction of inelastic scattering does not immediately destroy magnetoresistive and current-induced torques in nanostructures with two antiferromagnetic elements separated by a paramagnetic spacer. On the contrary, we find that the GMR ratio goes to zero smoothly for spacer

thicknesses larger than the phase coherence or inelastic scattering length. (Ab-initio calculations for Cr/Au/Cr antiferromagnetic spin-valves²⁶ demonstrate that there is an additional interface related contribution to antiferromagnetic GMR which is not captured by our toy model and is not limited by inelastic scattering in the spacer layer.) Since typical inelastic scattering lengths at room temperature ($\sim 10\text{nm}$) are much larger than the minimum paramagnetic spacer layer thicknesses required to make coupling between magnetic layers insignificant, inelastic scattering does not impose any practical limitation on GMR and current-induced torques in thin film based antiferromagnetic metal nanostructures.

Unlike the ferromagnetic case, current-induced torques in antiferromagnets do not follow simply from the approximate conservation of total spin angular momentum. Toy model calculations, as well as *ab initio* calculations for realistic systems²⁶, suggest that both GMR and current-induced torques tend to be somewhat weaker for very thin films in the antiferromagnetic case compared to GMR and spin transfer torques in ferromagnets. It seems natural to associate this property with the absence of grounding in a simple robust conservation law. A surprising and interesting property of ST physics in antiferromagnets is the property that torques act throughout the entire volume of the antiferromagnet in the phase coherent case. This property helps to compensate for the tendency toward somewhat weaker effects in very thin films. When inelastic scattering is introduced, spin-torques again act only over a finite thickness $\sim L_\phi$ within the antiferromagnets. Still the length scale over which the torque acts should be $\sim 10\text{nm}$, much longer than the atomic length scale over which spin torques act in ferromagnetic spin-torque structures.

As explained in earlier work⁹, ST effects in antiferromagnets are expected to be strongest when moment directions alternate in the direction of current flow. In the one-dimensional single channel model studied here, this is the only possibility. For real three-dimensional antiferromagnets this property requires particular orientations of current with respect to the crystal axes, or in thin film structures particular growth directions for the antiferromagnetic films which yield alternating ferromagnetic layers. It seems likely that the greatest obstacle to achieving interesting GMR and current-induced torques in purely antiferromagnetic circuits may be the difficulty in growing antiferromagnetic thin films with individual ferromagnetic layers that are not strongly compensated. Studies of the influence of magnetic disorder within ferromagnetic layers on GMR and ST physics require multi-channel Green's function calculations and will be the subject of future work.

This work was supported by the National Science Foundation under grants DMR-0606489, DMR-0210383, and PHY99-07949, by a grant from Seagate Corporation, and by the Welch Foundation. ASN was supported in part by Proyecto Mecesus FSM0204.

-
- * Electronic address: duine@phys.uu.nl;
URL: <http://www.phys.uu.nl/~duine>
- † Electronic address: haney411@physics.utexas.edu;
URL: <http://www.ph.utexas.edu/~haney411/paulh.html>
- ‡ Electronic address: alvaro.nunez@ucv.cl;
URL: <http://www.ph.utexas.edu/~alnunez>
- § Electronic address: macd@physics.utexas.edu;
URL: <http://www.ph.utexas.edu/~macdgrp>
- ¹ S. Washburn and R.A. Webb, Adv. Phys. **35**, 375 (1986).
 - ² R. Landauer, IBM J. Res. Dev. **1**, 223 (1957).
 - ³ M. Büttiker, Phys. Rev. Lett. **57**, 1761 (1986).
 - ⁴ M. Büttiker, IBM J. Res. Dev. **32**, 63 (1988).
 - ⁵ J. L. D'Amato and H.M.Pastawski, Phys. Rev. B **41**, 7411 (1990).
 - ⁶ K. Maschke and M. Schreiber, Phys. Rev. B **44**, 3835 (1991).
 - ⁷ H.U. Baranger and P.A. Mello, Phys. Rev. B **51**, 4703 (1995).
 - ⁸ P.W. Brouwer and C.W.J. Beenakker, Phys. Rev. B **51**, 7739 (1995).
 - ⁹ A.S. Núñez, R.A. Duine, P.M. Haney, and A.H. MacDonald, Phys. Rev. B **73**, 214426 (2006).
 - ¹⁰ Z. Wei, A. Sharma, A. S. Nunez, P. M. Haney, R. A. Duine, J. Bass, A. H. MacDonald, and M. Tsoi, cond-mat/0606462.
 - ¹¹ B. Michaelis and C.W.J. Beenakker, Phys. Rev. B **73**, 115329 (2006).
 - ¹² M. Baibich, M. Broto, A. Fert, F. Nguyen Van Dau, F. Petroff, P. Eitenne, G. Creuzet, A. Friederich, and J. Chazelas, Phys. Rev. Lett. **61**, 2472 (1988).
 - ¹³ J. Barnas, A. Fuss, R. E. Camley, P. Grünberg, and W. Zinn, Phys. Rev. B **42**, 8110 (1990).
 - ¹⁴ J.C. Slonczewski, J. Magn. Magn. Mater. **159**, L1 (1996).
 - ¹⁵ L. Berger, Phys. Rev. B **54**, 9353 (1996).
 - ¹⁶ S. S. P. Parkin, N. More, and K. P. Roche, Phys. Rev. Lett. **64**, 2304 (1990).
 - ¹⁷ S. Datta, J. Phys C: Condens. Matter **2**, 8023 (1990).
 - ¹⁸ A.S. Núñez and A.H. MacDonald, Solid State Comm. **139**, 31 (2006).
 - ¹⁹ C. Caroli, R. Combescot, P. Nozieres, and D. Saint-James, J. Phys. C: Solid State Physics **5**, 21 (1972).
 - ²⁰ S. Datta, *Electronic Transport in Mesoscopic Systems*, Cambridge University Press (1995).
 - ²¹ Zhen-Gang Zhu, Gang Su, Biao Jin, Qing-Rong Zheng, Phys. Lett. A **306**, 249 (2003).
 - ²² A. A. Yanik, G. Klimeck, and S. Datta, cond-mat/0605037.
 - ²³ Y. Meir, and N.S. Wingreen, Phys. Rev. Lett. **68**, 2512 (1992).
 - ²⁴ D. S. Fisher and P. A. Lee, Phys. Rev. B **23**, 6851 (1981).
 - ²⁵ M. Stiles and A. Zangwill, Phys. Rev. B **65**, 014407 (2002).
 - ²⁶ P.M. Haney, D. Waldron, A.S. Núñez, R.A. Duine, H. Guo, A.H. MacDonald, to be published.